Bulg. J. Phys. 34 (2007) 136–148

ULF Wave Index and Its Possible Applications in Space Physics

N. Romanova[1], **V. Pilipenko**[2], **N. Crosby**[3], **O. Khabarova**[2]

[1]Institute of the Physics of the Earth, Russia

[2]Space Research Institute

[3]Belgian Institute of Aeronomy

Received *20 May 2007*

Abstract. The solar wind-magnetosphere interaction has a turbulent character, which is not accounted for by commonly used geomagnetic indices and OMNI parameters. To quantify the level of low-frequency turbulence/variability of the geomagnetic field, IMF, and solar wind plasma, we have introduced ULF wave power indices. These simple hourly indices are based on the integrated spectral power in the band 2–7 mHz or wavelet power with time scales $\sim$ 10–100 min. The ground wave index has been produced from the data of global magnetometer arrays in the northern hemisphere. The interplanetary and geostationary wave indices have been calculated using magnetometer and plasma data from interplanetary and geosynchronous satellites. These indices have turned out to be useful for statistical analysis of various space weather problems. These indices enables one to examine easily the statistical correspondence between the ULF activity and interplanetary conditions. For example, the enhancements of relativistic electrons at the geosynchronous orbit were not directly related to the intensity of magnetic storms, but they correlated well with intervals of elevated ground ULF wave index. This fact confirmed the importance of magnetospheric ULF turbulence in energizing electrons up to relativistic energies. The interplanetary index has revealed statistically the role of the interplanetary turbulence in driving the magnetosphere by the IMF/solar wind. The application of this index to the analysis of conditions in the solar wind before magnetic storm onsets has shown that a weak irregular increase of the solar wind density is observed on average 2 days prior to storm commencement. The ULF index database for the period since 1991 is freely available via anonymous FTP for all interested researchers for further validation and statistical studies.

PACS number: 94.30.vf, 96.50.Ci

1 Introduction: The Necessity of Wave Indices

The interaction between the solar wind (SW) and terrestrial magnetosphere is the primary driver of many processes and phenomena occurring in the magnetosphere. This interaction has often been viewed using the implicit assumption of quasi-steady and laminar plasma flow. However, many of the energy transfer processes in the magnetospheric boundary regions have a sporadic/bursty character, and the observations have highlighted the importance of including the effects of turbulence as well [1,2]. The turbulent character of SW drivers and the existence of natural MHD waveguides and resonators in near-terrestrial space in the lower ULF frequency range ($\sim$ 1–10 mHz) ensures a quasi-periodic magnetic field response to forcing at the boundary layers. Therefore, much of the turbulent nature of plasma processes of SW-magnetosphere interactions can be monitored with ground or space observations in the ULF range.

The progress in understanding and monitoring the turbulent processes in space physics is hampered by the lack of convenient tools for their characterization. Various geomagnetic indices (Kp, Dst, AE, PC, ϵ, *etc.*) quantify the energy supply in certain regions of the coupled SW-magnetosphere-ionosphere system, and are used as primary tools in statistical studies of solar-terrestrial relationships. However, these indices characterize the steady-state level of the electrodynamics of the near-Earth environment. Till recent there was no index characterizing the turbulent character of the energy transfer from the SW into the upper atmosphere and the short-scale variability of near-Earth electromagnetic processes. At the same time, there are many space weather related problems, where even a rough proxy of the level and character of low-frequency turbulence, which might be coined a ULF turbulence index, is of key importance.

A new hourly turbulence index, using the spectral ULF power in frequency band 1–2 mHz to 8–10 mHz has been introduced in [3]. The wave power index characterizes the ground ULF wave activity on a global scale and is calculated from world-wide array of high-latitude stations data. The ground power index is augmented by interplanetary and geostationary ULF wave indices, as indicators of the turbulent state of the interplanetary space and magnetosphere. The set of wave power indices from ground, geostationary, and interplanetary monitors provides a researcher with a convenient and easy tool for the statistical study of the role of MHD turbulence in the solar wind-magnetosphere interactions. In this paper we test the significance of these ULF indices for the statistical studies of various aspects of the solar-terrestrial relationships and demonstrate their merits and disadvantages.

2 Algorithm of the ULF Wave Index

Algorithm of the ULF wave index [3] relies on the estimate of the ULF wave power $F_j = B_j(f)^2$ in the band Δf from f_L to f_H averaged over N_c components ($j = 1, 2$)

$$T = \frac{1}{N_c}\left[\Delta f \sum_j \int_{f_L}^{f_H} F_j(f)df\right]^{1/2}. \quad (1)$$

The signal component S of the spectral power is calculated similar to (1), but with the background spectral power $F^{(B)}(f)$ subtracted from the total spectral power $F(f)$, namely $F_j(f) \rightarrow F_j(f) - F_j^{(B)}(f)$. The background spectrum is determined as a least-square fit of the power-law spectral form $F^{(B)}(f) \propto f^{-\alpha}$ in a chosen frequency band. The spectral power below $F^{(B)}(f)$ is attributed to noise $N_j(f)$, so $T_j = S_j + N_j$. The final product is composed from the zoo of hourly ULF wave indices:

— Ground ULF wave index (T_{GR}, S_{GR})) is a proxy of global ULF activity. For its production, the algorithm selects the peak value of wave powers of 2 horizontal components from all the magnetic stations in the sector from 05 to 15 MLT (to avoid irregular nighttime disturbances), and in the latitudinal range from 60° to 70° geomagnetic latitudes;

— Geostationary ULF wave index (T_{GEO}, S_{GEO}) is calculated from 1-min 3-component magnetic data from GOES satellites to quantify magnetic fluctuations in the region of geostationary orbit;

— Interplanetary ULF wave index to quantify the short-term IMF variability (T_{IMF}, S_{IMF}) and solar wind fluctuations T_n is calculated from the 1-min data from the interplanetary satellites WIND, ACE. The data are time-shifted to the terrestrial bow shock ($\sim 15R_E$). Alternatively, the recent 1-min
OMNI database may be used;

— Additionally, we have applied the wavelet technique to estimate the integrated power of the SW density fluctuations W_n with time scales 4–128 min.

The histogram of the occurrence probability of log S_{GR} index is shown in Figure 1. The typical value of S_{GR} is about 10 nT. Further we demonstrate that a wide range of space physics studies benefits from the introduction of the ULF wave index.

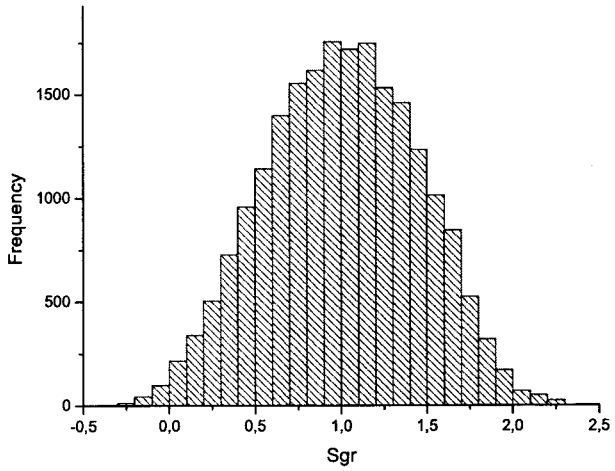

Figure 1. The occurrence probability of the log S_{GR} index.

3 Solar Wind/Magnetosphere Coupling

The turbulent/eddy viscosity of the SW flow passing the magnetosphere is controlled to a considerable extent by the level of upstream turbulence. However, the turbulence of the magnetosheath plasma which directly interacts with the magnetosphere, is significantly different for the conditions of quasi-parallel or quasi-perpendicular bow shock [4]. Nonetheless, the degree of coupling of the SW flow to the magnetosphere appears to be influenced by the level of SW/IMF turbulence upstream of the Earth [2]. The eddy viscosity concept predicts that the coupling to be lessened when the level of upstream turbulence is lessened. The effective Reynolds numbers of the SW and magnetosheath flows and that of the internal magnetospheric flows are very high, so the magnetosphere behaves as a turbulent high-Reynolds-number system. Therefore, the presence of turbulence inside and outside the magnetosphere should have profound effects on the large-scale dynamics of the system through eddy viscosity and diffusion.

Using the introduced ULF index T_{IMF}, here we verify the fact that when the SW is more turbulent, the effective degree of its coupling to magnetosphere is higher [2,5]. Auroral response, as characterized by hourly AE index, is compared with a strength of the SW driver, determined by the IMF B_z component, for the laminar and turbulent IMF (Figure 2). The IMF is considered noisy when T_{IMF} is high, and IMF is calm when T_{IMF} is low, or, equivalently, when the IMF hourly dispersion $\sigma > 2$ nT and $\sigma < 2$ nT. Comparison of median curves shows that under southward IMF ($B_z < 0$) AE nearly linear grows upon increase of the magnitude of B_z. However, for positive B_z the average AE values do not strongly depend on SW driver, but auroral response for the turbulent IMF is higher. This

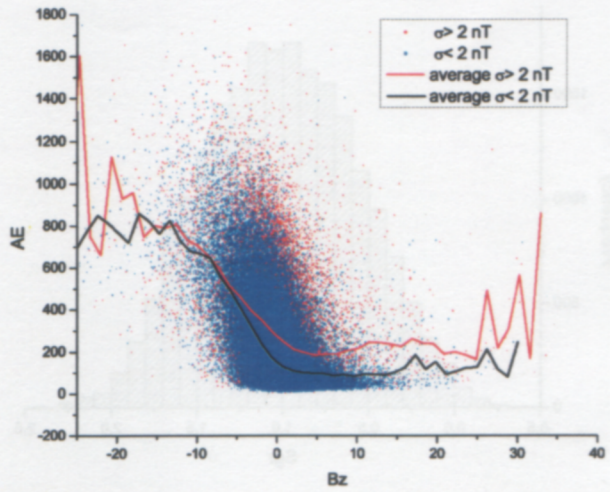

Figure 2. The dependence of auroral activity, as characterized by AE index, on the IMF driver (B_z) for laminar ($\sigma < 2$ nT) and turbulent ($\sigma > 2$ nT) IMF.

difference is most significant for northward IMF, when one expects the viscous interaction to be dominant over the reconnection. This comparison confirms that the magnetosphere is driven more weakly when the IMF turbulence level is low.

4 Statistical Properties of the IMF/SW Turbulence

The availability of interplanetary ULF index gives us a possibility to examine the relationship between the SW ULF turbulence and interplanetary parameters. We have analyzed hourly values of IMF, SW, and the interplanetary wave index. To reveal the significance of the IMF orientation on the interplanetary fluctuations we have divided all values into northward IMF events ($B_z > 0$) and southward IMF events ($B_z < 0$).

The correspondence between the interplanetary ULF index S_{IMF} and the SW velocity V (Figure 3a) has the following features. The northward (blue dots) and southward (red dots) events have the same dependence on the SW velocity. The correspondence between the IMF wave power and V has somewhat different character for slow SW ($V < 450$ km/s) and fast SW ($V > 450$ km/s). The statistical swamp of samples has a clear low cut-off boundary, which means that for a particular V the intensity of IMF fluctuations cannot be less than a certain value. This low boundary of possible ULF fluctuation intensity grows with increase of V.

On the other hand, there is an upper cut-off, which is F-independent, indicating that for any SW velocity the IMF ULF fluctuations cannot exceed some satu-

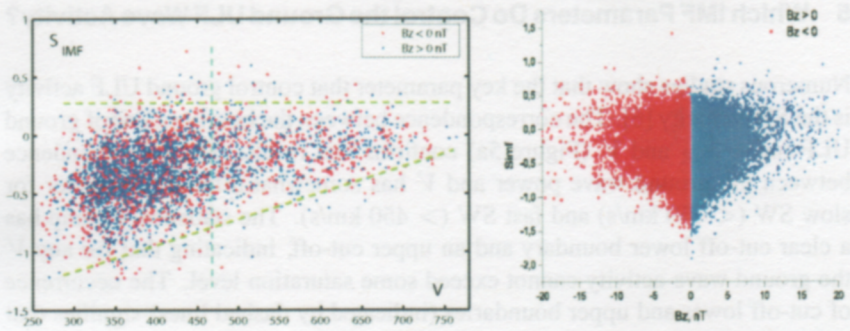

(a) (b)

Figure 3. Correspondence between the interplanetary ULF magnetic fluctuations, as characterized by log S_{IMF} index, and (a) SW velocity V for IMF $B_z > 0$ (blue) and $B_z < 0$ (red); and (b) IMF orientation B_z.

ration level. The occurrence of cut-off lower and upper boundaries (marked by dashed lines) signifies that the intensity of IMF fluctuations is within certain limits for any V. This result is to be interpreted by the theories of SW turbulence generation.

Is the SW velocity the only controlling factor of IMF wave turbulence, or may the IMF orientation be also of some importance for ULF variability? To answer this question we analyze the distributions of S_{IMF} index for positive and negative B_z values (Figure 3b). The distribution has turned out to be symmetric. Thus, the level of IMF turbulence does not depend on IMF north-south orientation.

Contrary to magnetic fluctuations, the plasma turbulence intensity, as characterized by the T_n index, does not depend on V (Figure 4a). The higher values of T_n generally correspond to larger magnitudes of IMF B_z component, but without any preference to northward or southward orientation (Figure 4b).

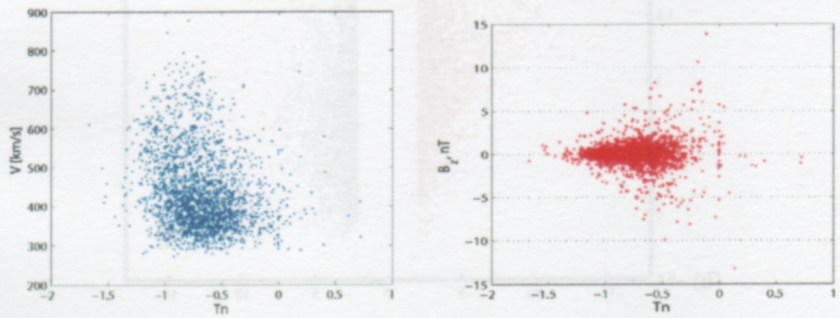

(a) (b)

Figure 4. Correspondence between the SW plasma fluctuations, as characterized by log T_n index, and (a) SW velocity V for IMF $B_z > 0$ and $B_z < 0$, and (b) IMF B_z.

5 Which IMF Parameters Do Control the Ground ULF Wave Activity?

Numerous studies show that the key parameter that control ground ULF activity is the SW velocity [6]. The correspondence between the hourly values of ground ULF index S_{GR} and V (Figure 5a) confirms this result. The correspondence between the ground wave power and V has somewhat different character for slow SW (< 450 km/s) and fast SW (> 450 km/s). The statistical swamp has a clear cut-off lower boundary and an upper cut-off, indicating that for any V the ground wave activity cannot exceed some saturation level. The occurrence of cut-off lower and upper boundaries (indicated by dashed lines) signifies that the intensity of ground fluctuations is within certain limits for any V. These statistical features should be understood in the frameworks of the theory of ULF wave excitation through the Kelvin-Helmholtz instability (KHI).

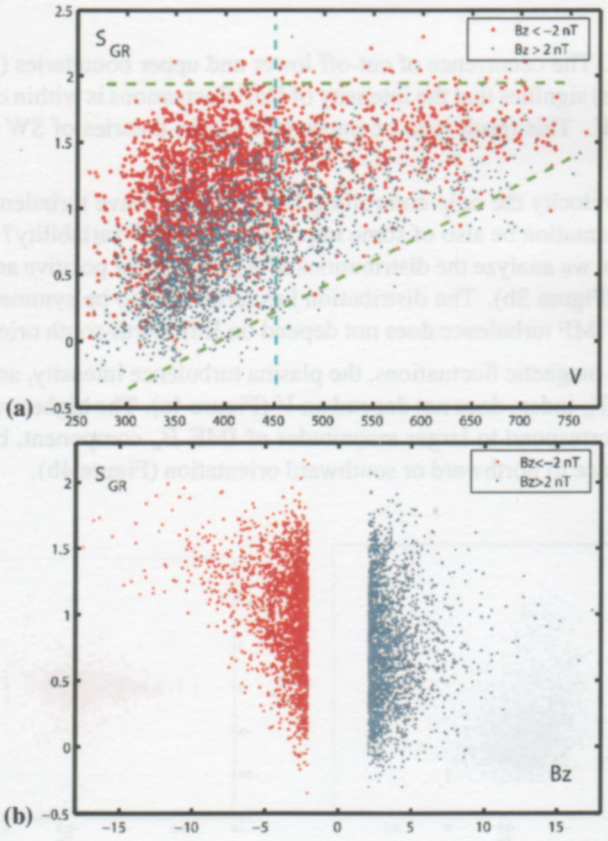

Figure 5. Correspondence between the global ground ULF activity, as characterized by log S_{sgr} index, and (a) SW velocity V for IMF $B_z > 0$ and $B_z < 0$, and (b) IMF B_z.

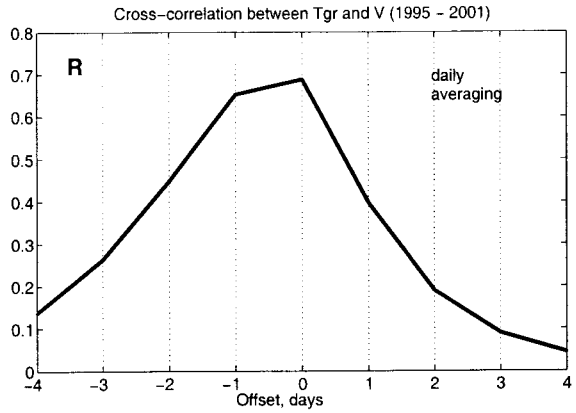

Figure 6. The coefficient of cross-correlation between T_{GR} and V.

In order to check whether the SW velocity is the only controlling factor of magnetospheric wave activity, we have separated all data samples into positive IMF events ($B_z > 0$) and negative IMF events ($B_z < 0$). Figure 5a shows that northward (blue dots) and southward (red dots) events have the same dependence on V, but, in contrast to the interplanetary fluctuations, under southward IMF the ground ULF wave activity is higher. The distribution of S_{GR} and B_z samples (Figure 5b) is also skewed: for $B_z < 0$ the ground wave power is generally higher than for $B_z > 0$. Thus, reconnection contributes into processes that stimulate the generation of ULF activity.

The results of the cross-correlation analysis of ground ULF activity, as characterized by T_{GR} index and SW parameters are given in Figure 6. The asymmetry of the cross-correlation function indicates that the increase of magnetospheric ULF activity starts earlier statistically than the increase of V. This may signify that the KHI is not the only mechanism of ULF wave generation, but the irregular SW plasma density enhancements preceding the occurrence of high-speed streams contribute also into ULF wave excitation [18]. Indeed, the SW V and N shows strong statistical anti-correlation (~ -0.65 between daily values), with peak value of cross-correlation function indicating that N precedes V by about 0.5 day (not shown).

6 IMF and SW Variability before Magnetic Storms

The SW density fluctuations with time scales $\sim$ 2–250 min are often observed many hours before magnetic storm onsets [7]. This fact has been verified statistically, using introduced wave indices. First, we have examined the change of the SW turbulence in the ULF frequency range. For that, we use the interplanetary ULF wave index T_n derived from the ACE plasma measurements. Figure 7

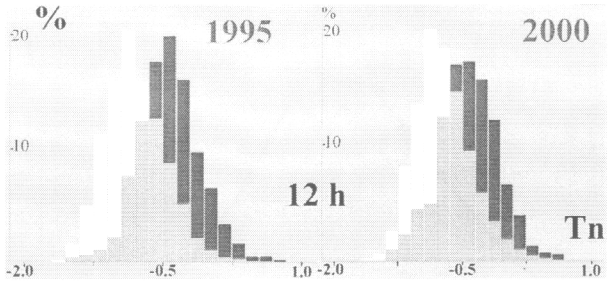

Figure 7. Statistical distributions of T_n index are compared: yearly distribution (white) and the distribution during 12-hour intervals before storm onsets (blue). Green color denotes intersection between them.

shows the histograms of T_n distributions during the entire year and during 12 hours intervals before storm onsets for solar maximum 1995 (left panel) and solar minimum 2000 (right panel). The statistics includes all the storms with intensity higher than $Dst < -50$ nT. This comparison shows a shift of the T_n distribution to higher values before storm onsets both during solar minimum and maximum. This enhancement becomes less evident for the 2 days interval before onset (not shown).

As a measure of lower frequency fluctuations we use the integrated wavelet power W_n with time scales from 4 min to 128 min. Figure 8 shows the comparison of the statistical distributions of W_n for the whole year and for the periods 12 hours before storm onsets for the 1995 (left-hand panel) and 2000 (right-hand panel). This comparison demonstrates the increase of the SW density fluctuation power of 12 hours before a storm onset, especially during solar maximum (1995). The same distribution for the time interval of 2 days shows a substantial decrease of the effect (not shown). Thus, the SW density becomes more turbu-

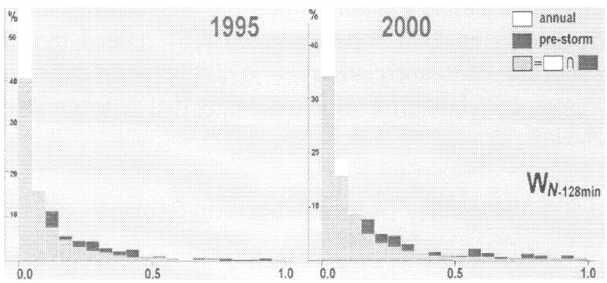

Figure 8. The low-frequency SW density fluctuations with time scales from $\sim$ 4 to $\sim$ 100 min, as estimated by the wavelet power W_n, during solar maximum (1995) and solar minimum (2000): yearly and 1 day prior to storm commencement (the same format as Figure 7).

lent and irregular about 1 day before the arrival of solar streams causing storm onset.

Previous solar wind works revealed the plasma density enhancements near the heliospheric current sheet (HCS) and high-speed corotating streams adjacent to the HCS plasma sheet [8]. Thus, a high plasma density and low velocity may be an indicator that a spacecraft and Earth are approaching the HCS region owing to the presence of naturally occurring high densities near the HCS and also to stream-stream compressive effects. The southward IMF, which eventually causes moderate storms, is related to the corotating stream interaction with the HCS and its plasma sheet. Although corotating stream/HCS plasma sheet interaction can create intense southward IMF, the field is typically highly fluctuating, thus providing only moderate or weak storms.

7 ULF Wave Index and Killer Electrons

Here we consider application of the ULF wave index to the problem of magnetospheric electron acceleration up to relativistic energies. The relativistic electron events are not merely a curiosity for scientists, but they can have disruptive consequences for spacecrafts [9,10]. Commonly, relativistic electron enhancements in the outer radiation belt are associated with magnetic storms [11,12], though the wide variability of the response and the puzzling time delay ($\sim$ 2 days) between storm main phase and the response has frustrated the identification of responsible mechanisms. Moreover, some electron events may occur even without magnetic storm or during very mild storms ($|Dst| \sim$ 20–40 nT). The example of such event on December, 1999 is shown in Figure 9. In this situation a high-

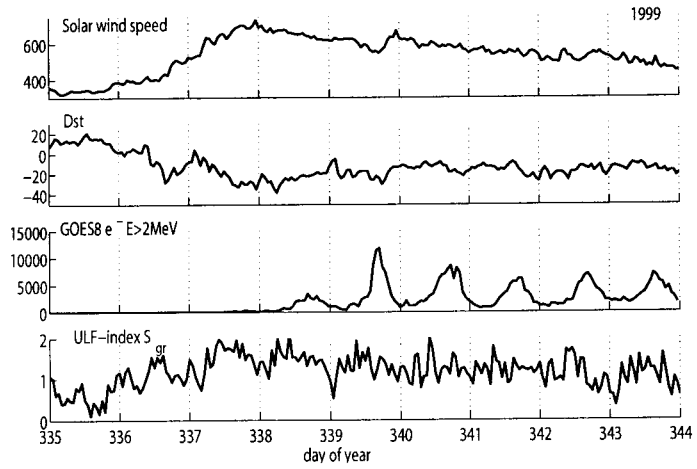

Figure 9. The electron event without magnetic storm observed at GOES-8 on December, 1999.

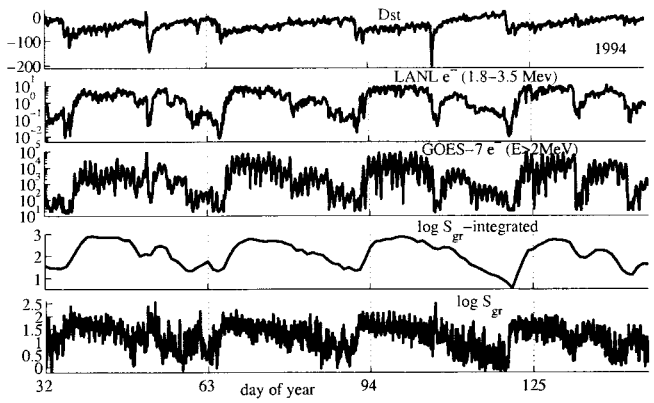

Figure 10. The comparison between the Dst index, electron fluxes at geostationary orbit measured by LANL J_e (cm^{2}keV-s-str)$^{-1}$ and GOES-7 J_e (cm^2-s-str)$^{-1}$, cumulative index $\langle S_{\rm GR}\rangle$ and ULF index $S_{\rm GR}$ during 1994.

speed solar stream occurs without a favorable B_z, and consequently without substantial storm (as measured by Dst index).

The efficiency of these non-identified mechanisms of energetic electron acceleration is strongly enhanced upon increase of V. Because the SW does not interact directly with magnetospheric electrons, some intermediary must more directly provide energy to the electrons. Rather surprisingly, ULF waves in the Pc5 band ($\sim$ few mHz) have emerged as a possible energy reservoir [13]: the presence of Pc5 wave power after minimum Dst was found to be a good indicator of relativistic electron response [14]. In a laminar, non-turbulent magnetosphere the killer electrons would not appear. Mechanism of the acceleration of $\sim$ 100 keV electrons supplied by substorms is revival of the idea of the magnetospheric geosynchrotron: pumping of energy into seed electrons is provided by large-scale MHD waves in a resonant way, when the wave period matches the multiple of the electron drift period [15,16]. However, this mechanism is not the only one, the local resonant acceleration upon interaction with high-frequency chorus emissions is claimed to be responsible for the relativistic electron occurrence [17].

The examples presented in [3] show that the increase of the relativistic electron fluxes up to 2-3 orders has occurred after weak storms, but the increase after strong storms is much shorter and less intense, whereas the correspondence with ULF wave activity is quite well for all events. A long-term persistent ULF activity is more important for electron acceleration than short-term ULF bursts though intense. Thus, the cumulative ULF index $\langle S_{\rm GR}\rangle = \int_{-\infty}^{t} S_{\rm GR}(t)\exp(-t/\tau)dt$, integrated over time pre-history $\tau \sim$ 2–3 days might be a better parameter than pure ULF index, as it illustrates the event showm in Figure 10. Indeed, the correlation of electron flux with integrated ULF-index

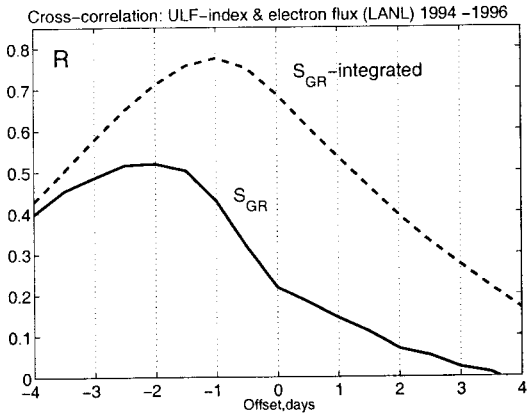

Figure 11. The cross-correlation function between the electron flux J_e $(\mathrm{cm^2keV\text{-}s\text{-}str})^{-1}$ at geostationary orbit measured by LANL and cumulative index $\langle S_{GR} \rangle$ (dashed) and ULF index S_{GR} (solid) during 1994.

increases substantially, from ~ 0.5 to ~ 0.8 (Figure 11). The cross-correlation function shows that the elevated level of ULF wave activity precede the peak of relativistic electron flux for about 2 days [19], whereas the same delay for the cumulative index is about 1 day. This increase of correlation, probably, implies the occurrence of a cumulative effect of some diffusion process. Thus, the long-lasting ULF wave activity is more important for the electron acceleration than just instant values.

8 Conclusions

The new ULF wave power index is a simple and convenient tool for the description of the turbulence of the SW-magnetosphere system and it can be applied to various space physics problems. Application of this index to the statistical examination of the SW plasma structure prior magnetic storms revealed medium-term precursors of severe space weather. The analysis based on the usage of these indices has elucidated the role of ULF turbulence in the magnetospheric field and particle response to SW/IMF forcing. Using the introduced indices, we have examined statistical relationships between the killer electrons and ULF activity. As expected, the correlation between electrons flux and the variations of $V$is high, but at the same time the interconnection between electrons flux variations and ULF pulsations also remains high throughout all phases of solar cycle, which indicates the mechanism of magnetospheric geosynchrotron (but not the only one!) contributes to the electron acceleration. Therefore, the ULF index should be taken into account by any adequate space radiation model. The ULF index database for the period since 1991 has freely been available via anonymous FTP (space.augsburg.edu/MACCS/ULF-index) for all interested researchers for further validation and statistical studies.

Acknowledgments

This study is supported by the INTAS grant 05-1000008-7978, and INTAS YSF 05-109-4661. We appreciate the help of O. Kozyreva and O. Chugunova in the index production.

References

[1] E.E. Antonova (2000) *Adv. Space Res.* **25** 1567-1570.

[2] J.E. Borovsky, H.O. Funsten (2003) *J. Geophys. Res.* **108** (A6) 1246, doi:10.1029/2002JA009601.

[3] O.V. Kozyreva, V.A. Pilipenko, M.J. Engebretson, K. Yumoto, J. Watermann, N. Romanova (2006) *Planetary Space Science*, doi:10.1016/j.pss.2006.03.013.

[4] N.N. Shevyrev, G.N. Zastenker (2005) *Planetary and Space Science* **53** 95-102.

[5] M.Yu. Goncharova, V.A. Pilipenko (2004) in: *Proc. of Conf. in memory Yu. Galperin 3-7 Feb., 2003 Auroral phenomena and solar-terrestrial relations*, Boulder, SCOSTEP, 134-141.

[6] M.J. Engebretson, K.-H. Glassmeier, M. Stellmacher, W.J. Hughes, H. Luhr (1998) *J. Geophys. Res.* **103** 26271-26283.

[7] O. Khabarova, V. Pilipenko, M.J. Engebretson, E. Rudenchik (2006) in: *Proc. of the 8-th International Conference on Substorms*, Canada, 127-132.

[8] B.T. Tsurutani, W.D. Gonzalez, A.L. Gonzales, F. Tang, J.K. Arballo, M. Okada (1995) *J. Geophys. Res.* **100** 21717-21733.

[9] N.V. Romanova, V.A. Pilipenko, N.V. Yagova, A.V. Belov (2005) *Kosmicheskie issledovanija (Space Research)* **43** 186-193.

[10] V. Pilipenko, N. Yagova, N. Romanova, J. Allen (2006) *Advances in Space Research* **37** 1192-1205.

[11] D.N. Baker, T. Pulkkinen, X. Li, S.G. Kanekal, J.B. Blake, R.S. Selesnick, M.G. Henderson, G.D. Reeves, H.E. Spence, G. Rostoker (1998) *J. Geophys. Res.* **103** 17279-17291.

[12] G.D. Reeves (1998) *Geophys. Res. Lett.* **25** 1817-1820.

[13] G. Rostoker, S. Skopke, D.N. Baker (1998) *Geophys. Res. Lett.* **25** 3701-3704.

[14] T.P. OBrien, R.L. McPherron, D. Sornette, G.D. Reeves, R. Friedel, H.J. Singer (2001) *J. Geophys. Res.* **106** 15533-15544.

[15] S.R. Elkington, M.K. Hudson, A.A. Chan (1999) *Geophys. Res. Lett.* **26** 3273-3276.

[16] A.Y. Ukhorskiy, K. Takahashi, B.J. Anderson, H. Korth (2005) *J. Geophys. Res.* **110** A10202, doi:10.1029/2005JA011017.

[17] N.P. Meredith, M. Cain, R.B. Home, R.M. Thome, D. Summers, R.R. Anderson (2003), *J. Geophys. Res.* **108** (A6) 1248, doi:10.1029/2002JA009764.

[18] N.G. Kleimenova, O.V. Kozyreva, J. Bitterly, J.J. Schott, P. Ivanova (2003) *Int. J. Geomagnetism and Aeronomy* **3** 229-244.

[19] I.R. Mann, T.P. O'Brien, D.K. Milling (2004) *J. Atmosph. Solar-Terr. Phys.* **66** 187-198,